Myosin and Paramyosin of *Caenorhabditis elegans* Embryos Assemble into Nascent Structures Distinct from Thick Filaments and Multi-Filament Assemblages

Henry F. Epstein, Douglas L. Casey, and Irving Ortiz

Department of Neurology, Baylor College of Medicine, 1 Baylor Plaza, Houston, Texas 77030

Abstract. The organization of myosin heavy chains (mhc) A and B and paramyosin (pm) which are the major proteins of thick filaments in adult wild-type *Caenorhabditis elegans* were studied during embryonic development. As a probe of myosin–paramyosin interaction, the *unc-15* mutation *e73* which produces a glu342lys charge change in pm and leads to the formation of large paracrystalline multi-filament assemblages was compared to wild type. These three proteins colocalized in wild-type embryos from 300 to 550 min of development after first cleavage at 20°C on the basis of immunofluorescence microscopy using specific monoclonal antibodies. Linear structures which were diversely oriented around the muscle cell peripheries appeared at 360 min and became progressively more aligned parallel to the embryonic long axis until distinct myofibrils were formed at 550 min. In the mutant, mhc A and pm were colocalized in the linear structures, but became progressively separated until they showed no spatial overlap at the myofibril stage. These results indicate that the linear structures represent nascent assemblies containing myosin and pm in which the proteins interact differently than in wild-type thick filaments of myofibrils. In *e73*, these nascent structures were distinct from the multi-filament assemblages. The overlapping of actin and mhc A in the nascent linear structures suggests their possible structural and functional relationship to the "stress fiber-like structures" of cultured vertebrate muscle cells.

THE processes underlying organization of myosin-containing thick filaments and actin-containing thin filaments into the regular myofibrillar arrays which define striated muscles are just beginning to be understood. Indeed, the assembly of the individual protein filaments although generally believed to result from self-assembly mechanisms, is likely to require additional proteins or their actions (Epstein and Fischman, 1991). Knowledge of the molecular nature and cellular location of the nascent structures in embryonic muscle is important for understanding myofibril assembly.

Arrays of thick and thin filaments are first detected in the vicinity of the plasma membrane of embryonic skeletal muscle cells in vitro and in ovo (Holtzer et al., 1957; Fischman, 1967; Kelly, 1969; Peng et al., 1981). Further developmental and morphological studies of these cells indicate that stress fiber-like structures (SFLSs)[1], bundles of actin filaments in association with multiple cytoskeletal proteins and membrane components, play an important role in the formation

of nascent myofibrillar structures (Kelly, 1969; Dlugosz et al., 1984; Peng et al., 1981; Schultheiss et al., 1990). Details of the mechanisms and molecular interactions by which SFLSs may act in early myofibril assembly are still unknown.

Recent work in the experimental genetic organisms *Drosophila* and *Caenorhabditis elegans* supports the hypothesis that membrane-associated cytoskeletal structures participate in the initiation and/or stabilization of nascent myofibrils, and inversely, myofibril assembly may stabilize membrane and extracellular interactions. Electron microscopic studies of developing flight muscles in *Drosophila* indicate that myofibril organization first occurs near the myotendon junction membrane although microtubules and not SFLSs appear to be involved (Reedy, M., and C. Beall. 1990. *Biophys. J.* 57:555a; Reedy, M., personal communication). The lethal *myospheroid* mutant which blocks muscle development in flies, is caused by a null mutation of integrin, a membrane protein which links the actin-based cytoskeleton and the extracellular matrix (MacKrell et al., 1988; Volk et al., 1990).

The significance of transmembrane connections is also emphasized by several studies in *C. elegans*. Nematode mutants producing no myosin heavy chain (mhc) A cannot assemble thick filaments and show alterations of muscle cell: hypodermal cell placement (Waterston, 1989). Similar phe-

---

Please address all correspondence to Dr. Henry F. Epstein, Department of Neurology, Baylor College of Medicine, 1 Baylor Plaza, Houston, TX 77030.

---

1. *Abbreviations used in this paper*: mhc, myosin heavy chain; MFAs, multi-filament assemblages; pm, paramyosin; SFLSs, stress fiber-like structures.

notypes can be produced by mutations in an extracellular protein (Goh and Bogaert, 1991) and the actin cytoskeleton-membrane linking protein vinculin (Barstead and Waterston, 1991). Reports from Waterston and his colleagues indicate that reaction with antibodies to integrin, mhc A, and vinculin show similar alignments about the muscle cell periphery before myofibril assembly in *C. elegans* embryos (Coutu, M. D., B. D. Williams, and R. H. Waterston. 1992. *Mol. Biol. Cell.* 3:215a).

Mutations in several genes of *C. elegans* produce multifilament assemblages (MFAs) with central paracrystalline paramyosin-containing structures and polar thick filament-like structures (Epstein et al., 1987; Waterston et al., 1980). Single charge change mutations in the *unc-15* paramyosin (pm) gene such as *e73* produce the largest MFAs and pm-deficient thick filaments whereas null mutants of the *myo-3* mhc A gene produce small MFAs and no individual thick filaments (Waterston, 1989). Two possible roles for MFAs could not be distinguished by the previous studies: nascent structures that are normally precursors for thick filament assembly but remain and grow in mutants because of the genetic block; or products of a pathway alternative to thick filament assembly that is favored by the mutant condition (Epstein et al., 1987). A special version of the latter model is favored by Gengyo-Ando and Kagawa (1991) in their analysis of the amino acid sequences of wild-type and the known *unc-15* mutations. In their model, MFAs are produced by mutations which favor pm–pm interactions and disfavor the normal mhc–pm interactions of thick filaments.

In the present report, we use well-characterized mAbs specific to mhc A, mhc B, and pm to study by immunofluorescence microscopy the expression and assembly of these well-studied thick filament proteins in embryos of *C. elegans*. In early wild-type and *e73* embryos, nascent linear structures are formed in which these proteins extensively colocalize in contrast to the myofibrils of later embryos and free-living forms in which the mutation disrupts mhc and pm interactions. MFAs form later than the nascent linear structures, at about the same times as the thick filament-containing A bands of the embryonic myofibrils. Actin overlaps with the mhcs and pm more closely in these nascent structures than in the later myofibrils. These results suggest that the nascent structures may be spatially related to SFLSs and contain myosin and pm assemblies different from the thick filaments of wild-type myofibrils and the mutant MFAs.

Materials and Methods

Nematode Strains and Growth

N2 (wild-type) and CB73 (*e73*, *unc-15 I*) strains of *C. elegans*, variety Bristol were used. Worms were grown on NGM plates seeded with *Escherichia coli*, OP 50 strain (Sulston and Brenner, 1974).

Monoclonal Antibodies

Mouse mAbs anti-mhc A 5-6, anti-mhc B 5-8, and anti-pm 5-23 have been previously described by this laboratory (Miller et al., 1983; Ardizzi and Epstein, 1987). The anti-actin mAb C4 was the generous gift of Dr. James Lessard of the University of Cincinnati (Lessard, 1988).

The reaction of the mAbs with homogenates of *C. elegans* embryos was analyzed by immunoblots of SDS-PAGE using alkaline phosphatase–derivatized affinity purified anti–mouse antibody for detection as described previously from this laboratory (Vybiral et al., 1992).

For immunofluorescence microscopy, the mAbs for the thick filament proteins were purified as IgGs (Miller et al., 1983) and then directly coupled to either FITC or tetramethylrhodamine-5-isothiocyanate (RITC). For example, 70 μg FITC were added to 1.0 mg IgG in a volume of 0.5 ml of 0.1 M sodium carbonate, pH 9.3, while stirring slowly at room temperature. The reaction mixture was incubated at 4°C in the dark. 162.5 μg RITC were added to 2.5 mg IgG in 1.0 ml, mixed, and incubated similarly. The products were separated from unreacted reagents by Sephadex G-25 gel filtration which was developed in PBS (0.29 M NaCl, 0.072 M KH$_2$PO$_4$, 0.228 M Na$_2$HPO$_4$, pH 7.2) (Pharmacia LKB Biotechnology, Piscataway, NJ). Using ϵ^{280} = 2.17 × 10^5 cm^2/mmol for IgG, ϵ^{494} = 7.2 × 10^4 cm^2/mmol for fluorescein, and ϵ^{537} = 1.07 × 10^5 cm^2/mmol for rhodamine, the derivatized mAbs used were determined to have 1–2 dye molecules conjugated per IgG molecule. For secondary localization of the anti-actin mAb, fluorescein-conjugated affinity purified goat anti–mouse IgG antibody (Cappel, Durham, NC) was used at a dilution of 1:100. mAb 5-6 was used at 2 μg/ml, and the other directly conjugated mAbs were used at 10 μg/ml.

Isolation of Embryos

Young adults which contain a small number of early embryos were raised at 20°C. The embryos were isolated by two methods. For untimed embryos, the gravid adults were collected in M9 buffer (Sulston and Brenner, 1974) and centrifuged (IEC Clinical, Needham Heights, MA) in 15-ml sterile tissue culture tubes (VWR Scientific Corp., Philadelphia, PA) at speed 3 for 5 min. The pelleted worms were resuspended in 10 ml of 1.25% sodium hypochlorite, 0.5 N NaOH, and shaken gently for 5–10 min to release the embryos and dissolve worm fragments. The free embryos were pelleted at setting 5 for 5 min, washed twice in cold M9 buffer, and resuspended in a minimal volume of buffer.

For timed embryos, washed worms were disrupted in the small rotor/holder of an Omni-Mixer (Dupont International, Newtown, CT) for 90 s at speed 7. The resulting free embryos and worm fragments were placed onto shallow depression well glass slides. Under a dissecting microscope, individual two-cell (first cleavage stage) embryos were removed with a drawn 50-μl capillary pipet and placed onto the surface of a 1% agar-coated slide. This stage lasts for only 10 min thus permitting precise timing. The embryos were incubated for specified times in a humidifying chamber at 20°C and collected in M9 buffer with a drawn pipet.

Preparation of Embryo Whole Mounts

Three different methods were used. For all three methods, acid-washed glass slides were coated by incubation with 0.2% gelatin, 0.1% poly-L-lysine (MW 150,000–300,000, Sigma Chem. Co., St. Louis, MO), and 0.01% chromium potassium sulfate, air dried, and then both incubation and drying were repeated.

In Method I, a drop of embryos suspended in M9 buffer was placed on a coated slide. A glass coverslip was placed on top, and the slide was immersed in liquid nitrogen for 10 s. The embryos were fractured while frozen by rapidly lifting off the coverslip with a razor blade. The slide was immediately immersed in 70% ethanol, incubated overnight at 4°C, and then incubated in 100% ethanol for 1 h at room temperature, air dried at 4°C, and stored until use.

In Method II, embryos were resuspended in 3% fresh paraformaldehyde in PBS and incubated for 10 min at room temperature. The fixed embryos were rinsed twice in cold doubly distilled H$_2$O and placed in 3 ml of cold (−20°C) methanol as rapidly as possible. The fixed embryos were stored up to 3 wk at −70°C in Eppendorf tubes (Brinkman Instruments, Inc., Westbury, NY).

In Method III, a drop of suspended eggs was placed on a coated slide, frozen and fractured, immersed first in methanol, and then in acetone, each at −20°C for 4 min. The slide was then washed gently with PBS/0.05% Tween-20. The embryos were covered by 100 μl of the PBS/Tween-20 and incubated overnight at 4°C. In Method III, embryos were always reacted with antibodies on the following day.

Antibody Labeling

Method I embryos, mounted on slides, were incubated in 50 μl undiluted normal goat serum (GIBCO BRL, Gaithersburg, MD) for 30 min at 37°C. The embryos were then rinsed twice with PBS and incubated with the first antibody diluted in PBS/10% goat serum for 1 h at 37°C. After two washes in PBS, the embryos were incubated identically with the second antibody and washed twice again. Almost all liquid was then removed from around the embryos, and a 10 μl drop of 1 mg/ml p-phenylenediamine in 90%
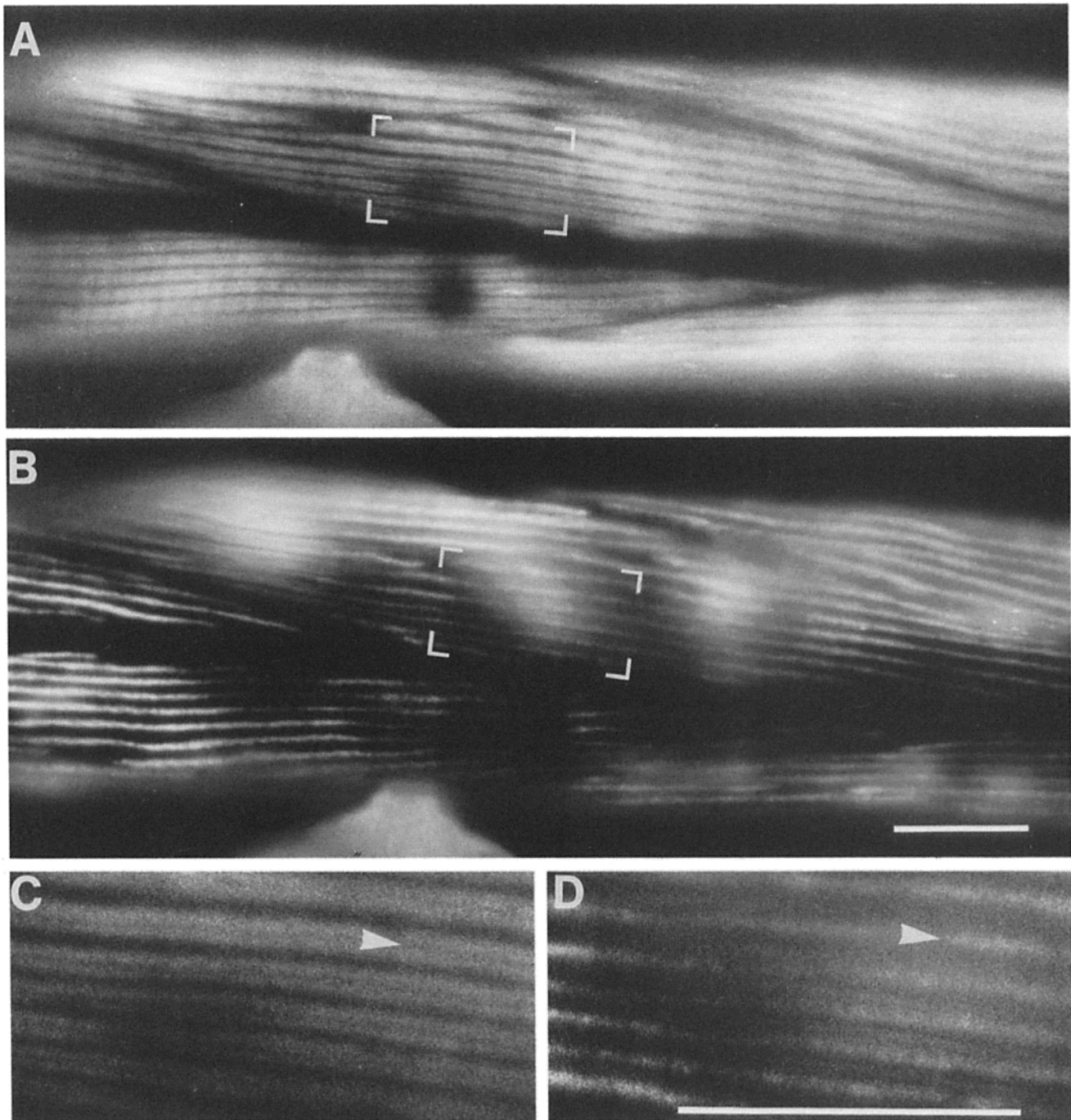
Figure 1. pm and mhc A in adult wild-type body-wall muscle. Nematodes were double-labeled with (*A*) fluorescein-coupled anti-pm mAb 5-23 and (*B*) rhodamine-coupled anti-mhc A mAb 5-6. *C* and *D* are magnifications of the enclosed areas in *A* and *B*, respectively. All images are of immunofluorescence photomicrographs in this and succeeding figures. The bars in all figures are 10 μm. The arrowheads in *C* and *D* represent the center of an A-band.

glycerol/10% PBS, 5 mM bicarbonate-carbonate, pH 8.0, was added. The specimens were sealed by placing a coverslip on top of them and nail polish around its edges. Method III embryos were treated similarly except that goat serum was not used in the incubations or washes.

Method II embryos were rehydrated through a 80–20%, 50–50%, 20–80%, 0–100% methanol-water series. They were incubated with the first antibody in PBS/0.05% Tween-20/2% goat serum for 2 h at room temperature or 4°C overnight. The eggs were washed five times in the PBS/Tween/goat serum and incubated with the second antibody in the same manner. The slides were then washed 3 × 20 min with the PBS/Tween/goat serum and then 3 × 5 min with PBS. The slides were then equilibrated through

a 20, 50, and 70% glycerol/PBS, pH 8.0 series, and then resuspended in 50–100 μl of 1 mg/ml p-phenylenediamine in 90% glycerol/10% PBS, 5 mM biocarbonate-carbonate pH 8.0. 10 μl of this mixture was added to clean slides and sealed as above.

Photomicroscopy

All photomicrographs were taken with a Zeiss Photomicroscope III (Zeiss, Gottingen, FRG) using Ilford XP1 and XP2 400 films (Ilford Inc., Paramus, NJ) at ASA 3200–6300 and developed with Ilford processing chemicals. Prints were made on Kodak Kodabrome II RC professional paper.
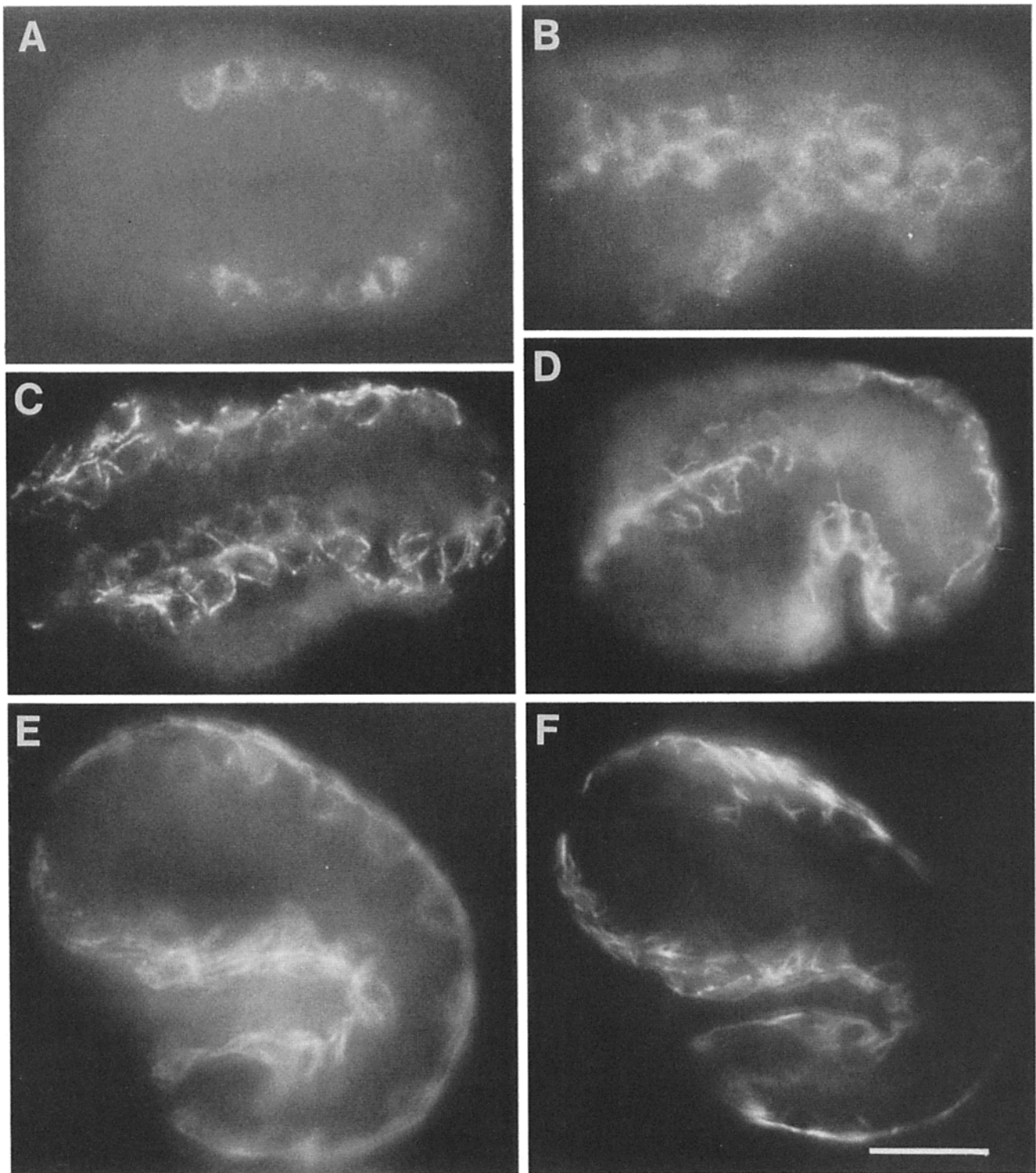
Figure 2. Muscle development in wild-type embryos. Rhodamine-coupled anti-mhc A mAb 5-6 was reacted with embryos at the following times after first cleavage: (*A*) 300, (*B*) 330, (*C*) 360, (*D*) 390, (*E*) 420, and (*F*) 450 min.

Results

Wild-Type Adult Muscle Assembles MHC A and Paramyosin into Striated Myofibrils

Mhc A and mhc B are assembled into discrete locations within the myofibrils of body-wall muscles in adult and larval forms; mhc A is localized to medial lines whereas mhc B is found in the flanking regions of the thick filament-containing A bands within the myofibrils (Miller et al., 1983). As a basis for our studies with wild-type and mutant embryos, we performed similar experiments using mAbs 5-6 and 5-23 which are specific to mhc A and pm, respectively (Ardizzi and Epstein, 1987).
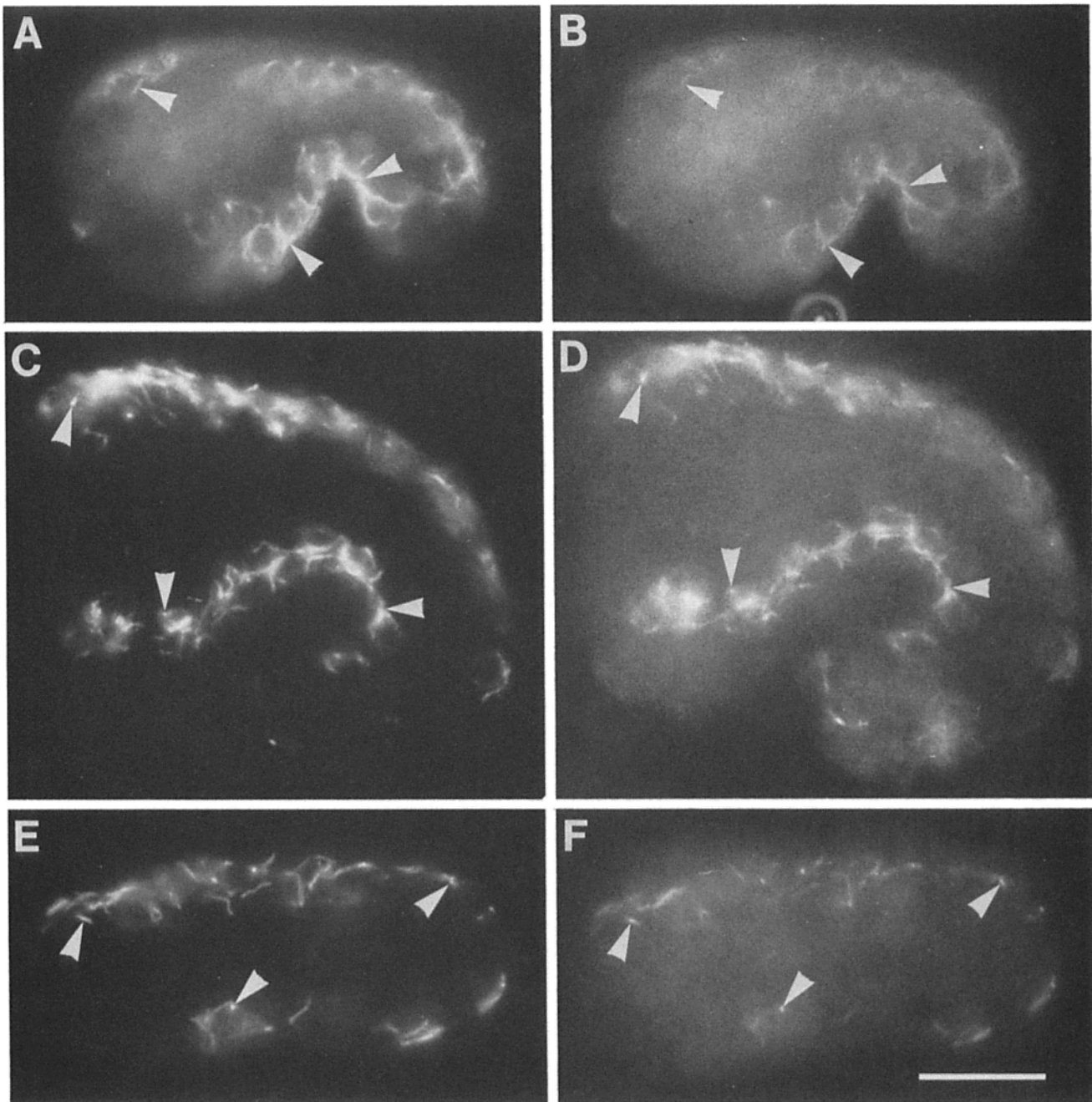
Figure 3. Controls for fixation and preparation of embryo whole mounts. Embryos were double-labeled with (*A, C,* and *E*) rhodamine-coupled anti-mhc A mAb and (*B, D,* and *F*) fluroescein-coupled anti-pm mAb. Fixation by (*A* and *B*) methanol/acetone, (*C* and *D*) 70% ethanol, and (*E* and *F*) 3% paraformaldehyde. The stages of embryos were (*A* and *B*) 420, (*C* and *D*) 450, and (*E* and *F*) 450 min. The arrowheads in this and succeeding figures are for reference to the same positions in companion micrographs.

All micrographs are shown at either a single standard magnification or a 2.5-fold higher magnification for enclosed areas and therefore, may be directly compared to one another. Both micrographs of all double-labeled specimens were photographed without change of focus for unbiased comparison.

All body-wall muscle cells and all A-bands within them doubly reacted with the two mAbs directly labeled with either fluorescein or rhodamine. As shown in Fig. 1, anti-mhc A labeled medial lines as previously reported. In contrast, anti-pm reacted more broadly. Surprisingly, central gaps in

the labeling of pm were seen in many but not all A-bands. The comparison at high magnification of the two labeling patterns (Fig. 1, *C* and *D*) is reminiscent of the differences between mhc A and B (Miller, et al., 1983). Identical observations were made with each antibody alone either directly labeled or unlabeled followed by labeled secondary antibody.

Embryonic Muscle Cells Assemble MHC A and PM into Nascent Structures Morphologically Distinct from Myofibrils

Fig. 2 shows the expression and organization of mhc A as
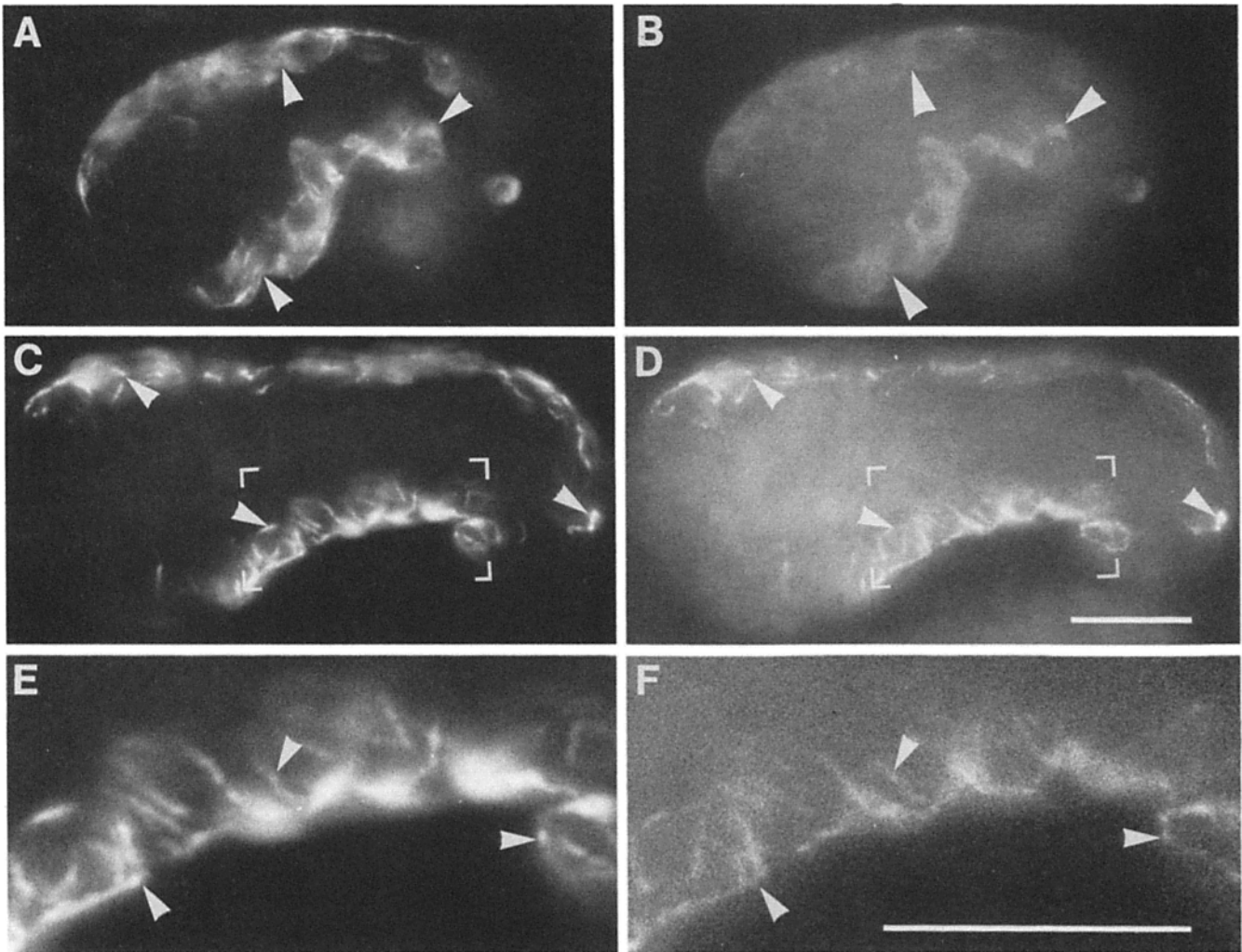
Figure 4. mhc A and mhc B in wild-type embryos. Embryos were double-labeled with (*A*, *C*, and *E*) rhodamine-coupled anti-mhc A and (*B*, *D*, and *F*) fluorescein-coupled anti-mhc B mAb 5-8. *E* and *F* are magnifications of enclosed areas in *C* and *D*, respectively. The stages of both embryos were 450 min.

a function of embryonic development. The embryos were collected by hand at the two-cell stage which synchronized them to within 10 min (Wood, 1988), and then incubated at 20°C for set times. This and other sets of timed embryos also served as a standard for assessing the stages of embryos in unsynchronized populations which were more convenient to use in some of the studies. mhc A was chosen as the definitive antigen because the reaction of rhodamine-derivatized mAb 5-6 consistently provided the strongest labeling by immunofluorescence microscopy and, therefore, was the most reliable indicator at the earliest stages.

Fig.2, *A* and *B* show embryos at 300 and 330 min, respectively. Cell proliferation is still occurring at these times, and not all of the 81 embryonic muscle cells have begun to express mhc A. The labeling appeared perinuclear and presumably, was cytoplasmic. At the level of resolution of immunofluorescence microscopy, it could not be ascertained whether mhc A was assembled or soluble.

Fig. 2, *C* and *D* show embryos at 360 and 390 min, respectively. The muscle cells have become organized into columns of the body wall. mhc A was clearly organized into discrete

linear structures, submicron to 3 μm in length. These linear structures appeared near the periphery of the cells and showed diverse orientations to the long axes of the embryos.

Fig. 2, *E* and *F* show embryos at 420 and 450 min, respectively. Many of the muscle cells have begun to elongate, and the linear structures in such cells have aligned parallel to the long axes. However, some cells were still at the rounded stage with peripheral linear structures as at the top of Fig. 2 *E*. It should be noted that none of the observed structures were large enough to contain the 10-μm long thick filaments of later larval and adult body-wall muscle cells (Mackenzie and Epstein, 1980).

As a test of the possibility that these linear structures were artifacts of fixation or preparation, 360–390 min embryos were prepared by three different methods and doubly labeled with mAbs to mhc A and pm as in Fig. 1. Fig. 3 shows that similar linear structures were observed by each of the methods. Remarkably, mhc A and pm exhibited very similar patterns over most of the muscle cells, however, clear focal differences were also observed.

To further assay the composition of the linear structures,
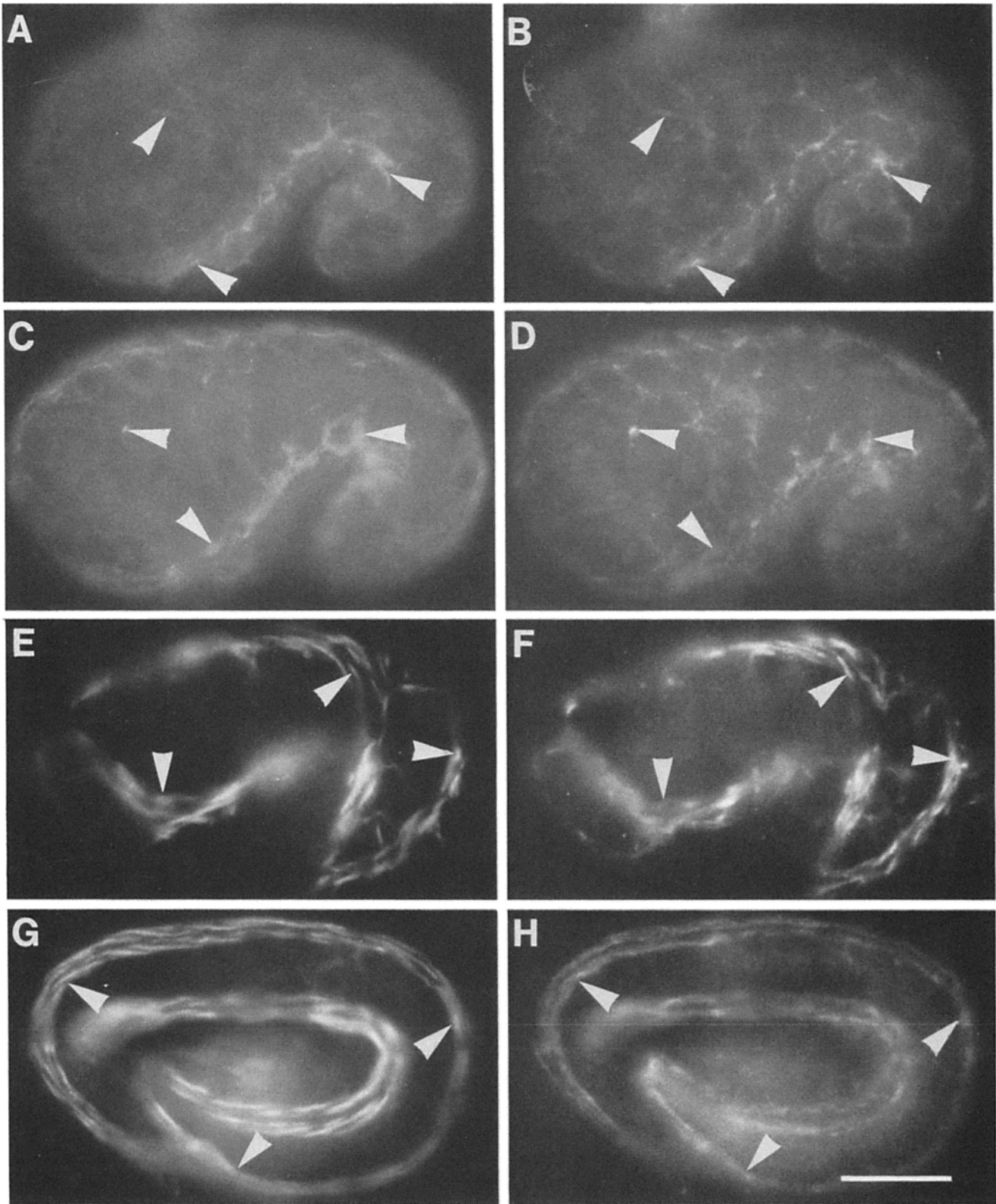
Figure 5. mhc A and actin in wild-type embryos. Embryos were double-labeled with (*A, C, E,* and *G*) rhodamine-coupled anti-mhc A mAb and (*B, D, F,* and *H*) indirectly fluorescein-labeled anti-actin mAb C4. The stages of embryos were (*A* and *B*) 360, (*C* and *D*) 360, (*E* and *F*) 450, and (*G* and *H*) 550 min.

A B C D E $M_R(kD)$

-229

-100

-42
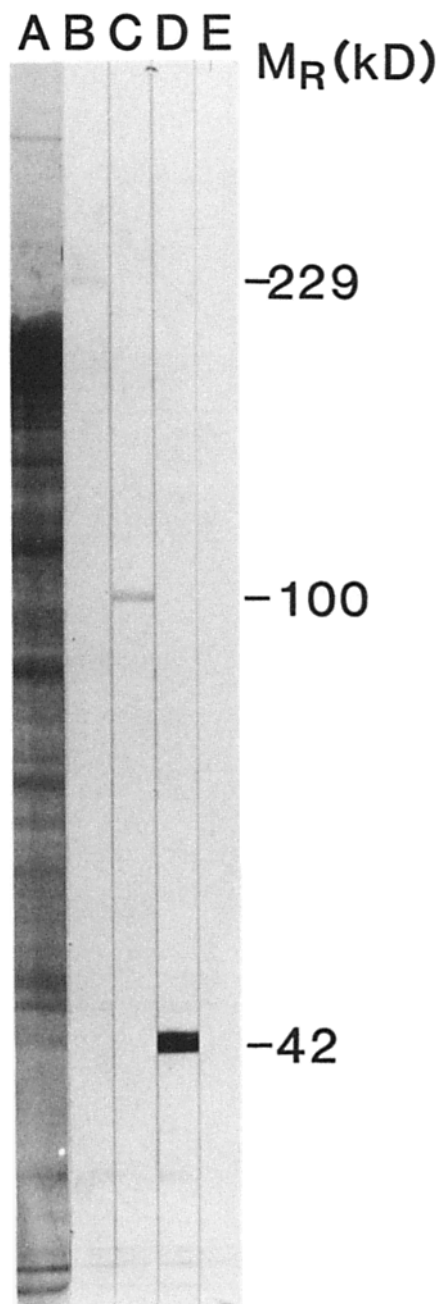
Figure 6. Specificity of mAbs by immunoblot analysis. 7.5% SDS-PAGE of mixed embryo homogenate was transferred to nitrocellulose and reacted with (*A*) Amido Schwarz for protein detection, (*B*) anti-mhc A at 2 μg/ml, (*C*) anti-pm at 10 μg/ml, (*D*) anti-actin at 10 μg/ml, and (*E*) secondary antibody alone. Antibody reactions were detected by alkaline phosphatase–linked affinity purified anti–mouse IgG antibody at 1:2,000.

embryos were doubly labeled with mAb 5-6 (mhc A) and either mAb 5-8 (mhc B), or mAb C4 (actin, courtesy of Dr. James Lessard) as shown in Figs. 4 and 5, respectively. The localizations of mhc A and B to the peripheral linear structures were extremely similar with only focal differences (Fig. 4, especially *E* and *F* at high magnification). Actin colocalized to a portion of the mhc A-containing areas in the linear structures and later aligning structures in contrast to its broader striated pattern at the myofibrillar stage (550 min or

threefold). The later results are consistent with the assembly of actin into thin filaments within the I-bands and possibly cytoskeletal structures whereas mhc A becomes restricted to the thick filaments of the A-bands. The limited extent of colocalization in the earlier stage raises the possibility that the nascent linear structures are related but are not identical to the cytoskeleton-like SFLSs observed in cultured vertebrate muscle cells.

As a test of the specificity of the reaction of these mAbs with embryos in contrast to adults or larvae, homogenates of mixed stage embryos were prepared by boiling in SDS/PAGE sample buffer and immediately separating the proteins on SDS/PAGE. Fig. 6 shows the immunoblot of such a separation reacted with the anti-mhc A, pm, and actin mAbs. The reaction of anti-mhc B could not be detected above background by alkaline phosphatase linkage. By comparison with the Amido Schwarz reaction (Fig. 6 *A*), the immunoreactive species (Fig. 6, *B–D*) were all relatively minor proteins in the embryos.

Interestingly, the order of amounts of proteins by weight detected in the embryos: actin > pm > mhc A or mhc A + mhc B is different than in adults where actin > mhc B > pm > mhc A (Harris and Epstein, 1977; Harris et al., 1977; Honda and Epstein, 1990). The reactions all appeared to be monospecific.

For most of the micrographs showing the reaction of embryos with fluorescein-conjugated mAbs, particularly the anti-mhc B and anti-pm mAbs, significant background fluorescence was observed. Several factors contributed to this problem. The weaker fluorescein signals required greater exposure times than the rhodamine images in general. Both kinds of signals were weaker in embryos than in larvae and adults because of the lesser amounts of filament proteins; the fluorescein was even more so. The signals with anti-mhc B and anti-pm mAbs were weaker than with anti-mhc A. However, these diffuse background reactions did not interfere with observing the muscle cell structures.

The e73 Mutation Disrupts Myofibril Assembly in Adults and Later Embryos

Fig. 7 shows the markedly disruptive effects of the *e73* mutation upon myofibrillar organization. The views and magnifications may be compared directly to those of Fig. 1. The locations of pm and mhc A bore little relationship to one another nor did they form any definite patterns. pm forms discrete structures, the MFAs, that are highly polymorphic and heterodisperse (Fig. 7 *C*) whereas mhc A appeared to fill the muscle cells amorphously (Fig. 7 *D*). The immunofluorescence detects many more and smaller MFAs than polarized light microscopy (Waterston et al., 1977). EM reveals that the pm forms the central paracrystalline regions of MFAs with mhc B-containing polar thick filaments and that mhc A is present in abnormal thick filaments which are not organized into regular myofibrillar arrays (Epstein et al., 1987; Waterston et al., 1977). Similar to other severely paralyzed strains, *e73* adults are significantly smaller than wild-type adults because their impaired locomotion interferes with feeding (Epstein et al., 1974). Because of the worm's thinness, the images involve superposition of muscle cells from two quadrants, and some MFAs will therefore falsely appear to cross cell boundaries.
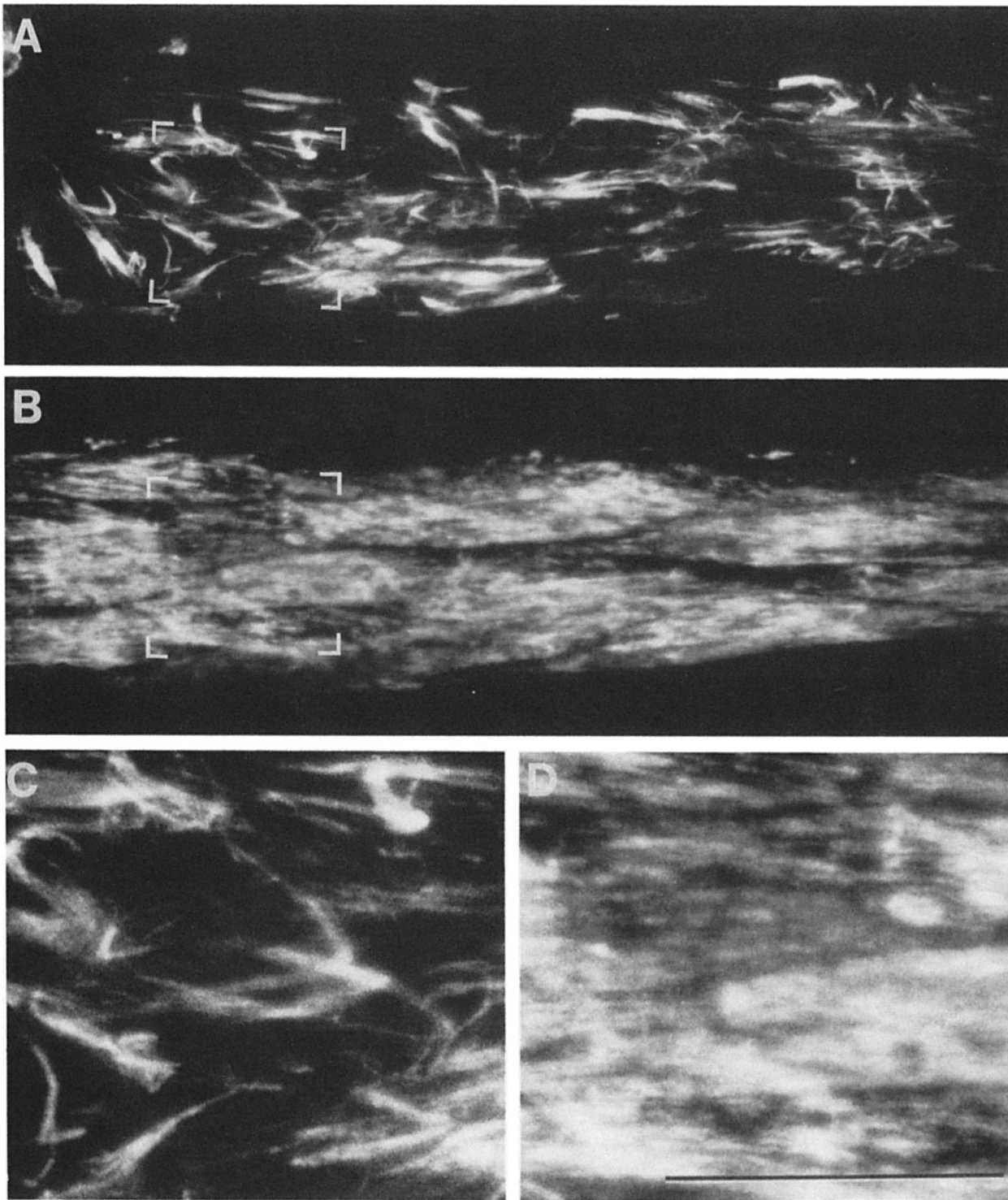
Figure 7. pm and mhc A in adult *e73* body-wall muscle. Adult *e73* nematodes were double-labeled with (*A*) fluorescein-coupled anti-pm mAb and (*B*) rhodamine-coupled anti-mhc A mAb. *C* and *D* are magnifications of the enclosed areas in *A* and *B*, respectively.

The *e73* disruption was evident in 2.5–3-fold (500–550 min) embryos (Fig. 8, *C* and *D*) with the pm localized in discrete bodies resembling in miniature the adult MFAs and the mhc A somewhat disarrayed. In contrast, wild-type embryos showed petite myofibrils in which pm and mhc A colocalized extensively (Fig. 8, *A* and *B*). The extent of spatial dissociation between mhc A and pm in the *e73* embryos is indicated by the MFAs being out-of-focus (Fig. 8 *D*) when the mhc

A-containing structures are in-focus (Fig. 8 *C*). In the wild-type embryos, the pm- and mhc-containing structures were in the same focal plane (Fig. 8, *A* and *B*).

Early Wild-Type and e73 Embryos Produce Very Similar Structures

Figs. 9 and 10 show that the nascent linear muscle structures of 360–390 min embryos are very similar in wild-type and
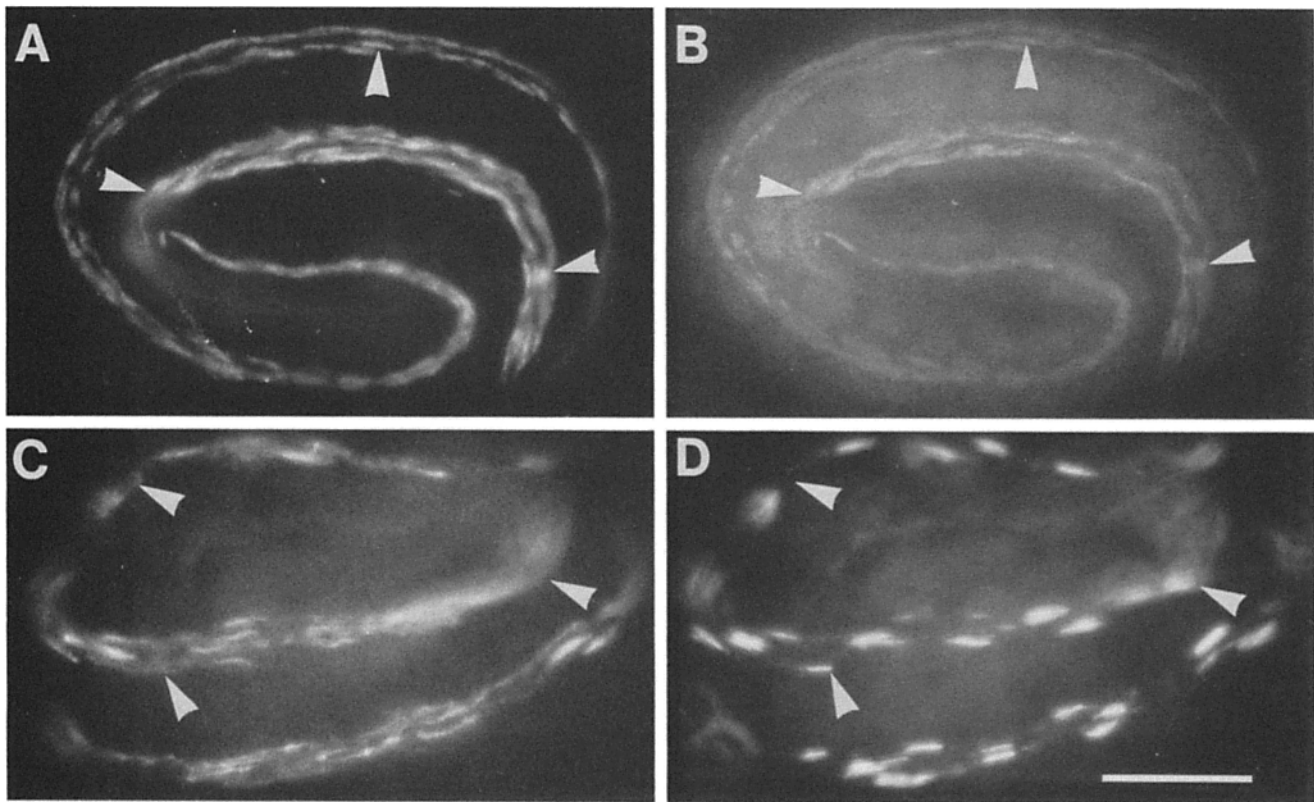
Figure 8. mhc A and pm in wild-type and *e73* embryonic myofibrils. 2.5–3-fold embryos of (*A* and *B*) wild-type and (*C* and *D*) *e73* strains were double-labeled with (*A* and *C*) anti-mhc A mAb and (*B* and *D*) anti-pm mAb. The stages of the embryos were (*A* and *B*) 500–550 and (*C* and *D*) 550 min.

e73. Comparison under high magnification of pm and mhc A labeling showed extensive colocalization in both wild-type (Fig. 9, *E* and *F*) and *e73* (Fig. 10, *E* and *F*). The disruptive effects appeared in 450-min mutant embryos when the linear structures began to align into myofibrils (Fig. 10, *C* and *D*). pm and mhc A clearly colocalized in a few areas but principally were in distinct, nonoverlapping structures within the mutant cells. The embryonic MFAs, therefore, began to form in *e73* at about the time as myofibrils coalesced in wild-type embryos and were distinct from the nascent linear structures.

Discussion

The thick filament proteins, mhc A, mhc B, and pm extensively colocalized through the early stages of muscle morphogenesis in wild-type *C. elegans* embryos. Four morphologically distinct stages were detected by immunofluorescence microscopy using specific mAbs. From 300 to 330 min, diffuse cytosolic staining of the early muscle cells with nuclear exclusion was apparent. From 360 to 390 min, distinct linear structures were detected around the peripheries of the muscle cells. From 420 to 450 min, the linear structures became progressively more aligned to the long axis of the embryos. From about 550 min, myofibrils with distinct A bands were apparent. Actin was similarly localized to the linear structures although its appearance was more punctate and its extent more limited than mhc A.

The *unc-15* pm mutation *e73*, a glu342lys single charge substitution, disrupts the interactions between mhc A and pm in adult thick filaments, produces myofibril disarray, and

favors the formation of highly polymorphic MFAs containing paracrystalline assemblies of pm (Epstein et al., 1987; Gengyo-Ando and Kagawa, 1991; Waterston et al., 1977). Similar disruption of myofibril assembly and formation of pm-containing MFAs was found in threefold *e73* embryos. The mutation did not affect colocalization of pm with mhc A in the linear structures of 360–390-min embryos, however, discrete localization of pm was detected in the next stage of progressive alignment.

The linear structures are termed nascent because they are the first structures recognized by immunofluorescence microscopy in nematode embryos. These nascent structures are distinct from the myofibrils of later stages because of the extensive colocalization of the three thick filament proteins, their close spatial relationship to actin-containing structures, and their arrangement about the peripheries of the muscle cells. The assembly of the thick filament proteins in the nascent linear structures must involve interactions distinct from those in wild-type thick filaments of later stages because of the lack of disruption by the *e73* mutation. The size (<5 μm in diameter) and rounded shape of the early embryonic muscle cells would preclude the formation of 10-μm long thick filaments of adult body-wall muscle cells (Gossett et al., 1982; Mackenzie and Epstein, 1980). It should be noted that even the myofibril-containing muscle cells of the threefold embryos would be too small to contain adult-size thick filaments (see Figs. 2 *F*; 5, *G* and *H*; 8, *A* and *B*).

An earlier report from this laboratory suggested that MFAs might represent precursors of thick filaments that were blocked by mutation (Epstein et al., 1987). Since the
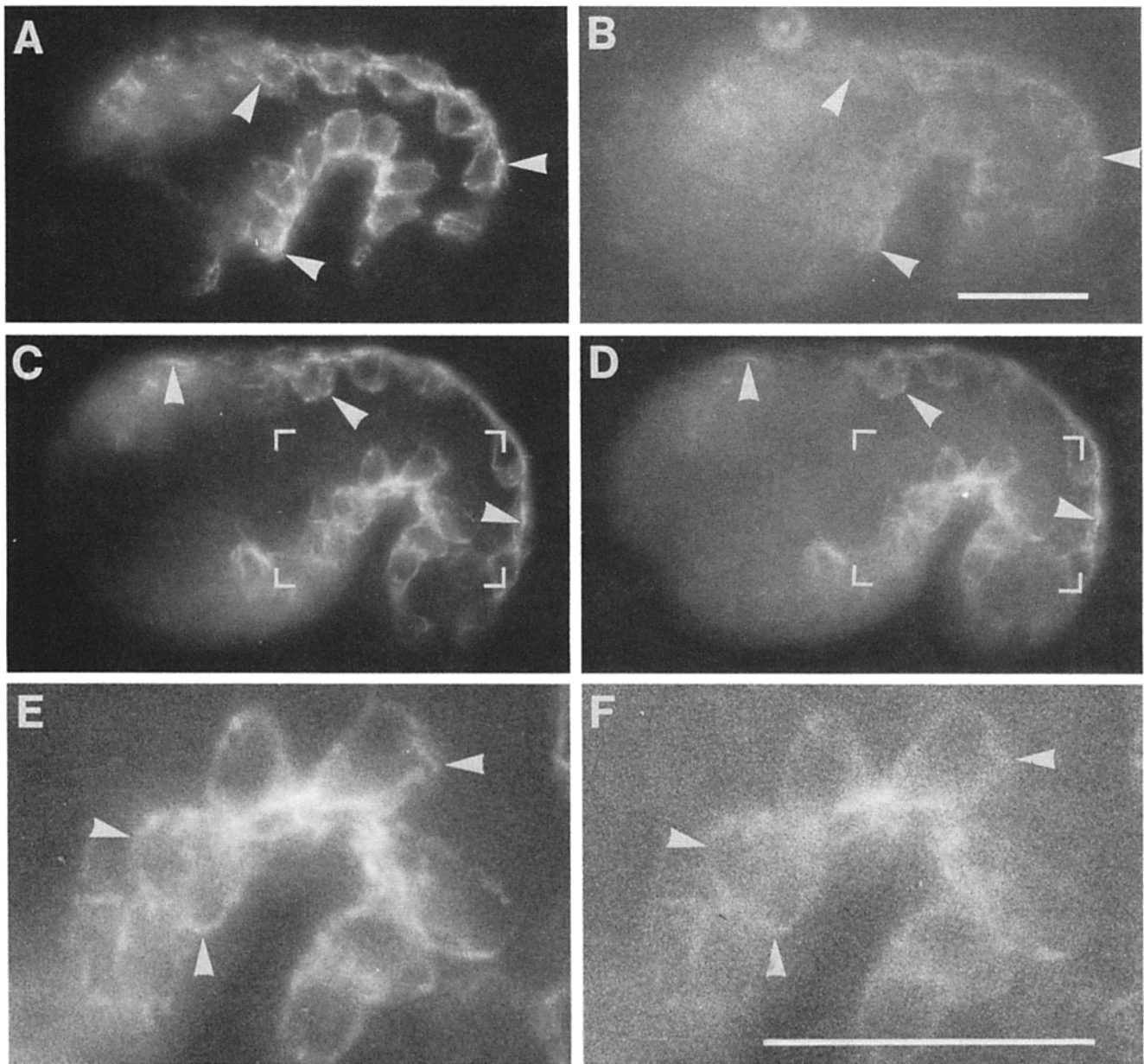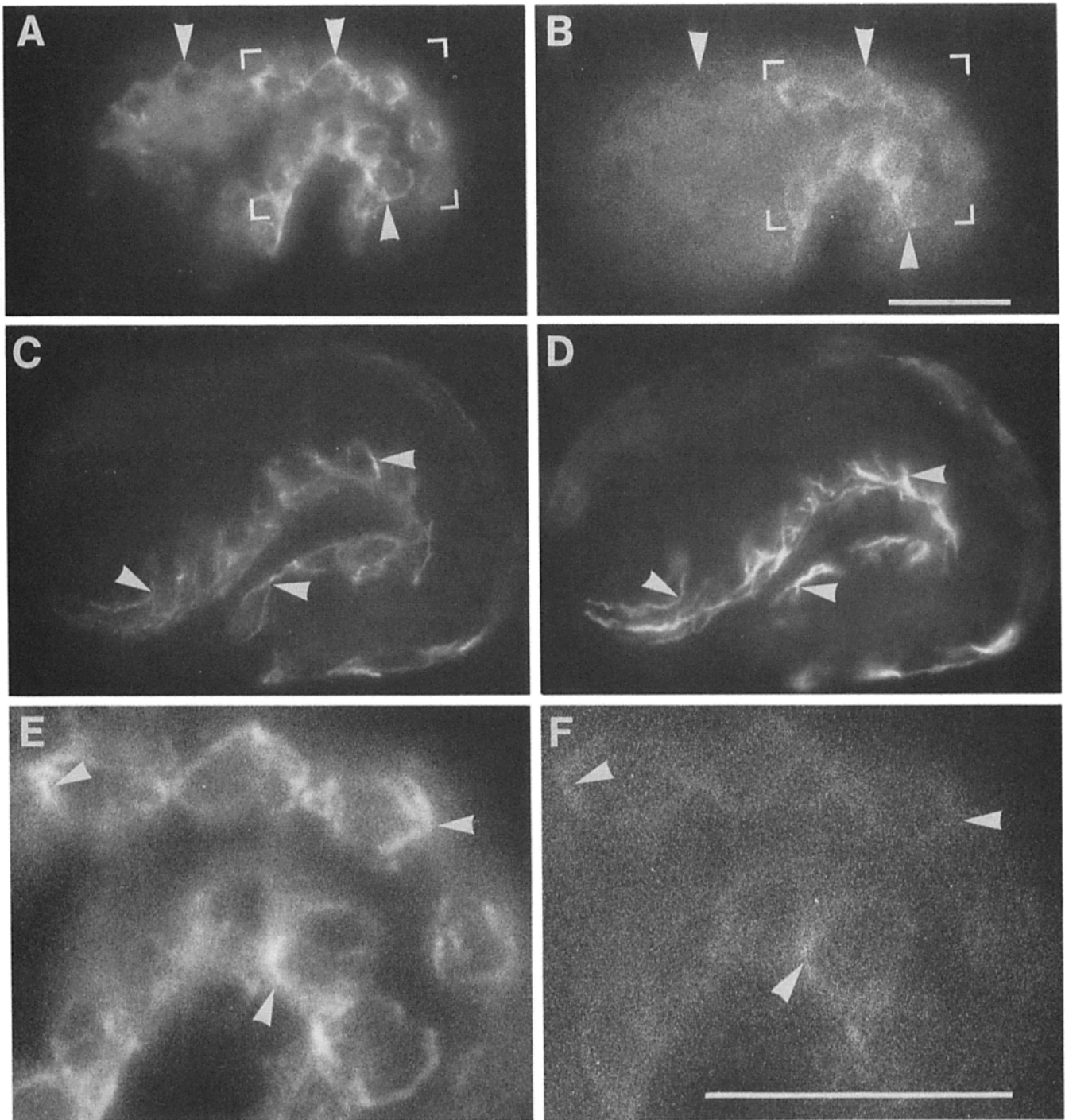
Figure 9. mhc A and pm in wild-type embryonic muscle development. Times after first cleavage were (*A* and *B*) 360 and (*C–F*) 420 min. Embryos were double-labeled with (*A* and *C*) rhodamine-coupled anti-mhc A and (*B* and *D*) fluorescein-coupled anti-pm mAb. *E* and *F* are magnifications of the enclosed areas in *C* and *D*, respectively.

nascent structures could also be candidates for a precursor in the assembly of embryonic thick filaments, the question as to whether nascent structures and MFAs are closely related or identical structures, is important. Our results found the MFAs and nascent structures to be distinct in several ways. The appearance of the nascent structures preceded that of the MFAs in *e73* embryonic muscle cells. MFAs did not contain mhc A in contrast to the nascent structures. MFAs did not first appear near the peripheries of the muscle cells as did the nascent structures. We conclude that the nascent structures and MFAs are not normal and mutant versions, respectively, of the same structure, but are distinct assemblies.

Genetic experiments from other laboratories indicate that the nascent structures and their association with the cell membrane may be necessary for normal muscle develop-

ment. In *C. elegans*, mutations in *deb-1* which encodes for vinculin, a putative linking protein between the actin cytoskeleton and the membrane, (Barstead and Waterston, 1991) and *mup-1* which is suggested to encode for an extracellular membrane component (Goh and Bogaert, 1991) produce similar phenotypes to those of mutations in *myo-3* which are deficient in mhc A and blocked at these early embryonic stages of myofibril assembly (Waterston, 1989). The spatial contiguity of actin-containing structures with the nascent structures containing the thick filament proteins that we have shown suggests a connection between our results and the findings of others (Coutu, M. D., B. D. Williams, and R. H. Waterston. 1992. *Mol. Biol. Cell.* 3:251a.). Although neither our results nor these experiments formally prove that the nascent linear structures are either precursors of thick filaments and myofibrils or scaffolds for their assembly, we

Figure 10. mhc A and pm in *e73* embryonic development. Times after first cleavage were (*A, B, E,* and *F*) 360 and (*C* and *D*) 450 min. Embryos were double-labeled with (*A* and *E*) rhodamine-coupled anti-mhc A mAb, (*B* and *F*) fluorescein-coupled anti-pm mAb, (*C*) fluorescein-coupled anti-mhc A mAb, and (*D*) rhodamine-coupled anti-pm mAb. *E* and *F* are magnifications of the enclosed areas in *A* and *B*, respectively.

present models in which the nascent structures play a necessary role in these assembly reactions in vivo (Fig. 11, *II* and *III*) as well as their being an alternative assembly of mhc A, mhc B, and pm (Fig. 11 *I*). These models may be tested in the future, possibly by genetic experiments. In contrast, the MFAs are most likely to represent a pathway of assembly of pm and other thick filament proteins which is alternative to normal thick filament assembly (Fig. 12 *II*).

The spatial association but not identity of actin-containing structures with the nascent linear structures suggests that SFLSs similar to those of developing vertebrate muscle cells (Kelly, 1969; Peng et al., 1981; Dlugosz et al., 1984; Schultheiss et al., 1990) may play important roles in early myofibril assembly in *C. elegans* embryos. More rigorous examination of this question by EM of serially sectioned embryos (Sulston et al., 1983) using fixation methods (Krieg et al.,

Myofibril Assembly Pathway

Model I: Parallel, Independent
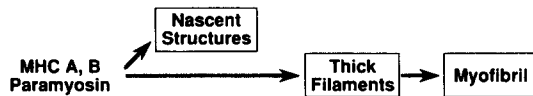
Model II: Precursor
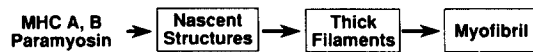
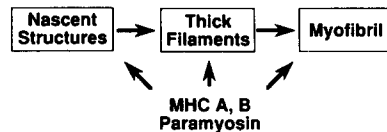**Model III: Mixed Models I, II**

Figure 11. Schematic diagram of different models for roles of nascent structures. In Model I, the nascent structures are alternative assemblies to thick filaments and myofibrils that are favored during embryonic myogenesis. In Model II, the nascent structures are part of the pathway for assembly of free thick filaments and myofibrils. In Model III, the thick filament proteins can be assembled into nascent structures, free thick filaments or thick filaments within myofibrils, and both nascent structures and free thick filaments are precursors of myofibrils.

1978) and staining procedures (White et al., 1986) that permit detailed visualization of subcellular structures such as SFLSs and muscle filaments is necessary. Localization of thick filament and cytoskeletal proteins with respect to specific structures could then be accomplished by EM of specific gold bead–labeled antibody complexes.

Understanding the process of myofibril assembly during muscle development in molecular and structural terms is an important goal of current research (for review see Epstein and Fischman, 1991). Mutations in several organisms including inherited human muscle diseases are important tools for dissecting physiological requirements for the assembly and maintenance of myofibrillar structures (for review see Epstein and Bernstein, 1992). In this report, studies of muscle development in wild-type and mutant embryos of *C. elegans* by immunofluorescence microscopy using specific monoclonal antibodies indicate that myosin and paramyosin

Multi-Filament Assemblages

Model I: Precursor to Thick Filament

Model II: Alternative to Thick Filament

Figure 12. Schematic diagram of different models for relationship of multi-filament assemblages and nascent structures. In Model I, MFAs are intermediates in the assembly of thick filaments. In Model II, MFAs are alternatives to thick filament assembly.

molecules first become organized into nascent structures distinct from the thick filaments of later myofibrils.

References

Ardizzi, J. P., and H. F. Epstein. 1987. Immunochemical localization of myosin heavy chain isoforms and paramyosin in developmentally and structurally diverse muscle cell types of the nematode *Caenorhabditis elegans. J. Cell Biol.* 105:2763–2770.

Barstead, R. J., and R. H. Waterston. 1991. Vinculin is essential for muscle function in the nematode. *J. Cell Biol.* 114:715–724.

Dlugosz, A. A., P. B. Antin, V. T. Nachmias, and H. Holtzer. 1984. The relationship between stress fiber-like structures and nascent myofibrils in cultured cardiac myocytes. *J. Cell Biol.* 99:2268–2278.

Epstein, H. F., R. H. Waterston, and S. Brenner. 1974. A mutant affecting the heavy chain of myosin in *Caenorhabditis elegans. J. Mol. Biol.* 90:291–300.

Epstein, H. F., I. Ortiz, and G. C. Berliner. 1987. Assemblages of multiple thick filaments in nematode mutants. *J. Muscle Res. Cell Motil.* 8:527–536.

Epstein, H. F., and D. A. Fischman. 1991. Molecular analysis of protein assembly in muscle development. *Science (Wash. DC).* 251:1039–1044.

Epstein, H. F., and S. I. Bernstein. 1992. Genetic approaches to understanding muscle development. *Dev. Biol.* 154:231–244.

Fischman, D. A. 1967. An electron microscope study of myofibril formation in embryonic chick skeletal muscle. *J. Cell Biol.* 32:557–575.

Gengyo-Ando, K., and H. Kagawa. 1991. Single charge change on the helical surface of the paramyosin rod dramatically disrupts thick filament assembly in *Caenorhabditis elegans. J. Mol. Biol.* 219:429–441.

Goh, P.-Y., and T. Bogaert. 1991. Positioning and maintenance of embryonic body wall muscle attachments in *C. elegans* requires the *mup-1* gene. *Development.* 111:667–681.

Gossett, L. A., R. M. Hecht, and H. F. Epstein. 1982. Muscle differentiation in normal and cleavage-arrested mutant embryos of *Caenorhabditis elegans. Cell.* 30:193–204.

Harris, H. E., and H. F. Epstein. 1977. Myosin and paramyosin from *Caenorhabditis elegans*: biochemical and structural properties of wild-type and mutant proteins. *Cell.* 10:709–719.

Harris, H. E., M.-Y. Tso, and H. F. Epstein. 1977. Actin and myosin-linked calcium regulation in the nematode, *Caenorhabditis elegans.* Biochemical and structural properties of native filaments and purified proteins. *Biochemistry.* 16:859–865.

Holtzer, H., J. Marshall, and H. Finck. 1957. An analysis of myogenesis by the use of fluorescent antimyosin. *J. Biophys. Biochem. Cytol.* 3:705–723.

Honda, S., and H. F. Epstein. 1990. Modulation of muscle gene expression in *Caenorhabditis elegans*: differential levels of transcripts, mRNAs, and polypeptides for thick filament proteins during nematode development. *Proc. Natl. Acad. Sci. USA.* 87:876–880.

Kelly, D. E. 1969. Myofibrillogenesis and Z-band differentiation. *Anat. Rec.* 163:403–426.

Krieg, C., T. Cole, U. Deppe, E. Schierenberg, D. Schmitt, B. Yoder, and G. von Ehrenstein. 1978. The cellular anatomy of embryos in the nematode *Caenorhabditis elegans. Dev. Biol.* 65:193–215.

Lessard, J. L. 1988. Two monoclonal antibodies to actin: one muscle selective and one generally reactive. *Cell. Motil. Cytoskeleton.* 10:362–369.

Mackenzie, J. M., Jr., and H. F. Epstein. 1980. Paramyosin is necessary for the determination of nematode thick filament length *in vivo. Cell.* 21:747–755.

Mackrell, A. J., B. Blumberg, S. R. Haynes, and J. H. Fessler. 1988. The lethal *myospheroid* gene of *Drosophila* encodes a membrane protein homologous to vertebrate integrin β subunits. *Proc. Natl. Acad. Sci. USA.* 85:2633–2637.

Miller, D. M., I. Ortiz, G. C. Berliner, and H. F. Epstein. 1983. Differential localization of two myosins within nematode thick filaments. *Cell.* 34:477–490.

Peng, H. B., J. J. Wolosewick, and P.-C. Cheng. 1981. The development of myofibrils in cultured muscle cells: a whole-mount and thin-section electron microscopic study. *Dev. Biol.* 88:121–136.

Schultheiss, T., Z. Lin, M.-H. Lu, J. Murray, D. A. Fischman, K. Weber, T. Masaki, M. Imamura, and H. Holtzer. 1990. Differential distribution of subsets of myofibrillar proteins in cardiac nonstriated and striated myofibrils. *J. Cell Biol.* 110:1159–1172.

Sulston, J. E., and S. Brenner. 1974. The DNA of *Caenorhabditis elegans*. *Genetics.* 77:95–104.

Sulston, J. E., E. Schierenberg, J. G. White, and J. N. Thomson. 1983. The embryonic cell lineages of the nematode *C. elegans*. *Dev. Biol.* 110:64–119.

Volk, T., L. I. Fessler, and J. H. Fessler. 1990. A role for integrin in the formation of sarcomeric cytoarchitecture. *Cell.* 63:525–536.

Vybiral, T., J. C. Winkelmann, R. Roberts, E.-H. Joe, D. L. Casey, J. K. Williams, and H. F. Epstein. 1992. Human cardiac and skeletal muscle spectrins: differential expression and localization. *Cell Motil. Cytoskeleton.* 21: 293–304.

Waterston, R. H. 1989. The minor myosin heavy chain, mhc A, of *Caenorhabditis elegans* is necessary for the initiation of thick filament assembly. *EMBO* *(Eur. Mol. Biol. Organ.) J.* 8:3429–3436.

Waterston, R. H., R. M. Fishpool, and S. Brenner. 1977. Mutants affecting paramyosin in *Caenorhabditis elegans*. *J. Mol. Biol.* 117:679–697.

Waterston, R. H., J. N. Thomson, and S. Brenner. 1980. Mutants with altered muscle structure in *Caenorhabditis elegans*. *Dev. Biol.* 77:271–302.

White, J. G., E. Southgate, J. N. Thomson, and S. Brenner. 1986. The structure of the nervous system of the nematode *Caenorhabditis elegans*. *Phil. Trans. R. Soc. Lond. B.* 314:1–340.

Wood, W. B. 1988. Embryology. *In* The Nematode *Caenorhabditis elegans*. W. B. Wood, editor. Cold Spring Harbor Laboratory, Cold Spring Harbor, NY. 215–241.